

See discussions, stats, and author profiles for this publication at: <https://www.researchgate.net/publication/231376109>

A Conjugated Polymer Network Approach to Anticorrosion Coatings: Poly(Vinylcarbazole) Electrodeposition

ARTICLE *in* INDUSTRIAL & ENGINEERING CHEMISTRY RESEARCH · SEPTEMBER 2010

Impact Factor: 2.59 · DOI: 10.1021/ie100813t

CITATIONS

23

READS

91

3 AUTHORS:



[Antonio Francesco Frau](#)

British School of Valencia

7 PUBLICATIONS 48 CITATIONS

[SEE PROFILE](#)



[Roderick B Pernites](#)

University of Houston

30 PUBLICATIONS 548 CITATIONS

[SEE PROFILE](#)



[Rigoberto C. Advincula](#)

Case Western Reserve University

334 PUBLICATIONS 7,238 CITATIONS

[SEE PROFILE](#)

A Conjugated Polymer Network Approach to Anticorrosion Coatings: Poly(vinylcarbazole) Electrodeposition

Antonio F. Frau, Roderick B. Pernites, and Rigoberto C. Advincula*

Department of Chemistry and Department of Chemical and Biomolecular Engineering, University of Houston, Houston, Texas 77204-5003

The fabrication and characterization of poly(vinylcarbazole) (PVK)-conjugated polymer network (CPN) anticorrosion coatings on flat surfaces, steel coupons or indium tin oxide (ITO) glass substrates, is reported. Electrochemical deposition methods (potentiostatic and potentiodynamic) were employed by anodic oxidation of the carbazole side units in the PVK chains, resulting in electrodeposition of a cross-linked or network macromolecular structure. This is different from traditional conjugated polymer (CP) coatings made up of mostly linear species derived from direct electropolymerization of small molecule monomers. The coating composition was characterized by attenuated total reflection infrared spectroscopy (ATR-IR) and photoelectron spectroscopy (XPS). Atomic force microscopy (AFM) allowed morphological comparison between the coatings in terms of deposition technique and surface roughness. Electrochemical impedance spectroscopy (EIS) was subsequently carried out on PVK-coated steel coupons to evaluate the performance of such coatings in an accelerated corrosion environment. The deviation from the ideal (i.e., perfectly dielectric) capacitor-like behavior and Bode plot data suggested that the CPN approach of electrodeposited PVK coatings resulted in very good protection against weathering of engineering metals.

1. Introduction

The corrosion of a material may be defined as its irreversible oxidative reaction with its environment, usually resulting in degradation of its properties. For metals, it may be viewed as a reverse extractive metallurgy; that is, corrosion is the process by which metals return to their oxide forms, a favorable chemical reaction.¹ It is one of the main structural destructive processes resulting in huge economic losses, especially in the aerospace, automotive, and petroleum industries. As there is not much that can be done to alter the weathering of structural (active) metals in natural environments, corrosion-control strategies are simply focused on slowing the rate of the corrosion process.² It is estimated that its annual cost and control is approximately 4% of a developed country's gross domestic product; for the United States alone, this amounts to ~\$300 billion per year.³

A common procedure is to apply a "primary" protection layer, which serves as a barrier between the metal and its environment. This delays the rate at which water, oxygen, or ions from the environment reach the metal surface. On the other hand, an "active coating" ("secondary" protection) consists of a material that can interact chemically or electrochemically with the metal, altering its corrosion behavior. So far, the most effective anticorrosion coatings for active protection of metals are chromate-containing systems.^{4,5} However, strict environmental regulations will eventually ban the use of all Cr(VI)-containing compounds in corrosion-protection systems. The need for the development of nonchromate, environmentally friendly surface treatments is urgent as mandated by the Environmental Protection Agency (EPA).⁶

Because the corrosion of a structural metal is an electrochemical phenomenon, electrochemical techniques are required to evaluate, understand, and prevent surface attack of aggressive environments on the metal surface. One of the most commonly used tools for evaluation is electrochemical impedance spec-

troscopy (EIS). It gives an accelerated measure of the resistance of a coating to ion transport phenomena and can thus give further long-term insight on corrosion-related issues. It measures the impedance response of the system as an AC potential is applied, spanning from a few mHz to 10–100 kHz where the $V(t)$ – $I(t)$ relationship (perturbation–response) is linear or pseudolinear within small ranges.^{7,8} The impedance Z , for a given pulse ω , is recorded in terms of its magnitude $|Z|$ and phase angle ϕ . The information that one can attain with $Z(\phi)$ is the tendency of an electrochemical system to impede the flow of an alternating electrical current. EIS spectra are modeled using mathematically equivalent electrical circuits and their elements (resistor, capacitor, etc.).^{9–12} Thus, using EIS, it is possible to probe the long-term phenomena of ion transport and variations in internal morphology in anticorrosion coatings as directly deposited on an electrode metal surface.

Other than electro-optical device applications, conducting polymers (CPs) are known to have practical applications as electrical capacitors, sensors, anodes for fuel cells, and in the preventative photodegradation of electrodes. They have been extensively investigated as anticorrosion protective coatings and have been applied to a variety of metal surfaces as first suggested by the late MacDiarmid.^{13–15} CPs consist of π -conjugated chains containing electrons delocalized along the polymer backbone and are capable of charge carrier generation (electrons and holes). As organic semiconductors, they can be synthesized both chemically and electrochemically and can be doped and converted into more electrically conductive forms.^{16–18} It has been observed that most CPs can be electrochemically produced by anodic oxidation¹⁹ (electropolymerization) on an electrode, enabling one to directly obtain a coating on a surface like indium tin oxide (ITO), gold, steel, etc. The anodic process involves both polymerization and subsequent deposition of the polymer via potentiostatic, potentiodynamic, or galvanostatic methods.²⁰

Like metals, doped CPs are electrically conducting with a defined Fermi energy level E_f , which can be modulated by doping.^{21,22} One might wonder why they could be useful as anticorrosion materials. Oxidized CPs (p-doped) usually display

* To whom correspondence should be addressed. Tel.: (713) 743-5151. E-mail: radvincula@uh.edu.

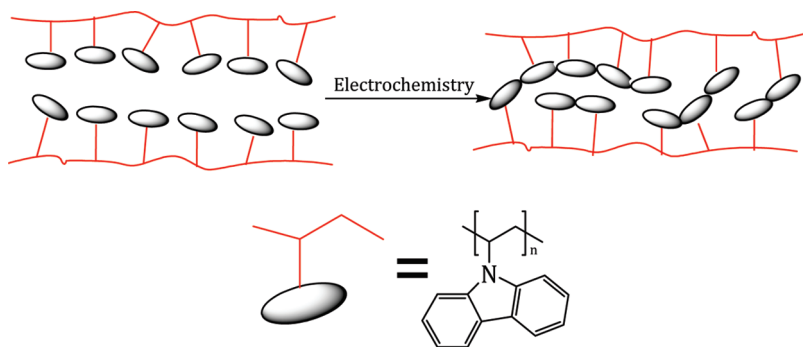


Figure 1. Schematic representation of the precursor polymer approach to CPN films: the precursor polymer has an electroactive unit (such as PVK in this example), which, upon electrochemical oxidation, can polymerize to give an extended π -conjugated polymer network through both inter- and intramolecular connectivity.

lower E_f values and, subsequently, higher work functions than engineering metals such as Fe, Ti, Al, etc. Therefore, when CPs and the metal surface are combined as a galvanic couple, the electron flows from the metal to the CP, producing a so-called Schottky barrier at the metal–semiconductor junction. Scanning Kelvin probe studies have shown that such a barrier arises from a p-type, CP/metal interface: as-protected metals show ennobled behavior in anticorrosion functions.²³ These electronic interactions are strongly influenced by the quality of the electrical contact between the CP and the metal, which in turn is influenced by adhesion and/or the presence of an oxide layer. The impervious weathering resistance of a coating is supposed to furnish a barrier against ion mobility at the metal interface, an increase of the electrolyte resistance within the local electrochemical cells that form on the surface. Thus, the metal surface preparation, method of coating deposition, and metal coating adhesion should be important considerations. In principle, further improvement of anticorrosion performances can be achieved by carefully choosing the polymerizable monomer and/or the dopant ion in electropolymerization-based techniques.²⁴ Corrosion inhibitors can also be incorporated as dopant anions, wherein the CP functions as an inhibitor-releasing coating upon reduction.² Several studies have addressed the influence of the dopant ion on corrosion behavior.^{25–29} “Smart” coatings^{30–32} release the inhibitor-anion on demand, that is, when damage to the coating triggers metal oxidation and/or polymer reduction.²⁷ The released anion can then act as second physical barrier to prevent penetration of aggressive ions²⁹ or inhibit oxygen reduction, for example, Cu-rich cathodic secondary phases in an Al alloy.²⁷ The approach may be particularly valuable for metals where passivity is difficult to achieve, for example, Al alloys in neutral, chloride-containing solutions.³³

Most CPs used in corrosion protection are linear polymers classified as polyanilines (PANI), polyheteroaromatics, and poly(phenylene vinylene)s.¹ PANI, poly(pyrrole) (PPy), or PANI composites on iron or steel in particular are quite popular.^{34–39} Thiophene and hydrazine derivatives, on the other hand, offer remarkable tendency to inhibit corrosion of metals in acid solutions.^{40–44} The use of CP films or CP-containing paints for corrosion protection of Zn,⁴⁵ Zn-coated steel,⁴⁶ Cu,⁴⁷ and Mg alloys⁴⁸ has also been described recently. There have been a few reports on the use of PANI for corrosion protection of Al and its alloys.^{49–51} Recently, several accounts of corrosion studies involving PPy or PPy composites on iron or steel were also discussed.^{52–56} However, a major drawback of electropolymerized CPs is their poor film-forming properties. This has been a perennial problem with respect to their application as coatings, because of the poor morphology and processing conditions that must be overcome for direct deposition of, say,

heteroaromatic or electroactive monomers for thin film coatings. Other attempts to improve film formation involved loading up with nanosized objects such as inorganic nanoparticles. Shchukin et al.⁸ used a layer-by-layer (LbL) approach for assembling poly(ethylene imine)/poly(styrene sulfonate) onto silica (SiO_2) particles. Such nanoparticles were subsequently imbibed with benzotriazole, a known corrosion inhibitor, and embedded in a sol–gel matrix. Other groups have also reported an LbL strategy on nonflat surfaces.⁵⁷

In the past, the Advincula group has demonstrated the deposition of high-quality, optical, ultrathin film coatings of CPs through a precursor polymer approach forming conjugated polymer network (CPN) films (Figure 1) (see Supporting Information).^{58,59}

They have reported on the synthesis and electrochemical deposition of “passive” polysiloxane-precursor derivatives of thiophene and pyrrole by either cyclic voltammetry (CV) or potentiostatic methods to form a highly cross-linked polymer film of polythiophene (PTh) and polypyrrole (PPy), respectively.⁶⁰ Moreover, it is also possible to synthesize “active” precursor polymers in which the polymer backbone itself is π -conjugated and displays electro-optical activity.⁶¹ These polymers can be directly electrodeposited from an electrolyte solution or coated directly to the electrode substrate first and then electrochemically oxidized.^{62,63} Basically, a precursor polymer by design contains pendant electroactive monomer units. Chemical or electrochemical oxidation results in a CPN film having both inter- and intramolecular cross-linkages via the pendant monomer units. Copolymerizing with electroactive monomers (small molecules) at various compositions enables control on the degree of cross-linking and linear polymer formation.⁶² The electrodeposition and electrochemical grafting of a carbazole containing precursor polymer (copolymer) with an “active” conjugated polyfluorene backbone onto ITO was previously reported.⁶⁴ The electro-active carbazole side group facilitated electrodeposition forming oligocarbazole links. The reaction occurs through a radical cation mechanism (Supporting Information). Thus, carbazole (Cbz) and polycarbazole (PCbz) derivatives such as poly(9-vinylcarbazole) or PVK are susceptible to electropolymerization and subsequent p-doping, which are similar to PANI and PPy. They have found viable applications in organic photoconductors, electrochromic, and electroluminescence devices because of their good hole-transport properties.⁶⁵ In principle, CPN films of oligo- and polycarbazole units can be easily deposited on a suitable working electrode such as ITO or steel. It should be noted that the HOMO–LUMO band gap of PVK can be tuned by means of CV, and, generally speaking, its oxidation potential (ca. +1.1 V vs SHE)⁶⁶ stands in the range of potentials displayed by the most common CPs

used for anticorrosion purposes, for example, PPy (-0.1 to $+0.3$ V), PANI ($+0.4$ to $+1.0$ V), and PTh ($+0.8$ to $+1.2$ V).^{67–69} The protection offered by self-assembled films of Cbz and *N*-vinylcarbazole against Cu corrosion in NaCl solution was recently studied.⁷⁰ The corrosion-protection studies using PVK on other metal surfaces, however, have not been carried out at all. By applying a CPN-driven approach, PVK can be considered a viable material whose potential anticorrosion capabilities on engineering metals may result in improved and efficient performance.

In this work, we have set out to fabricate CPN films of PVK by electrochemistry with the intent of evaluating their film-forming and anticorrosion properties. As mentioned, although carbazole-based conducting polymers are well-known electro-optical materials, their use as anticorrosion-protection material is yet to be explored. To date, no work has been done in this direction, although PVK-based films may be as promising as PANI.^{34–44} A coating electrodeposition protocol was rationally explored for flat surfaces to achieve films for characterization and testing. The chosen surfaces were ITO and stainless steel in which chemical and morphological information could be retrieved (from PVK-coated ITO and steel substrates) and anticorrosion behavior evaluated (from PVK-coated steel substrates). Film characterization was done through electrochemical (EIS) and nonelectrochemical techniques (FTIR, XPS, and AFM) to evaluate the chemical composition, film thickness, and surface morphology. Film performance, from EIS data on the potentiodynamic-deposited (i.e., CV-driven) coating, showed good ion transport blocking properties, according to accelerated corrosion tests. They also exhibited efficient corrosion resistance on steel coupons used as a model metal substrate.

2. Experimental Section

2.1. Materials and Substrate Preparation. All the materials were used as received unless otherwise specified. Dichloromethane (CH_2Cl_2) was freshly distilled over calcium hydride and collected immediately prior to use. PVK ($M_w \approx 72\,000$) and tetrabutylammonium hexafluorophosphate, TBAP (98%), analytical grade, were purchased from Aldrich Chemical Co. and used without further purification. Steel coupons (Corus Research, Development & Technology, The Netherlands) were cut into 1×2 cm pieces and cleaned in 10% $\text{NaOH}_{(aq)}$ at 70°C for 10 min to remove the protective oil, then quickly rinsed in water and isopropanol, followed by drying under N_2 stream and storing in vacuo until needed. Tin-doped indium oxide, ITO ($\text{In}_2[\text{Sn}_x]\text{O}_{3-y}$, one side coated on glass, sheet resistance $\leq 30 \Omega \text{ cm}^{-2}$) was used as substrate for analytical (IR, XPS) characterization of the coatings. For its surface activation, 1 \times 3 cm slides were cut and sonicated in isopropanol (10 min), hexane (10 min), and toluene (10 min), then dried under N_2 stream. Subsequent plasma-cleaning (3.5 min) afforded hydroxylated surfaces, which were stored in vacuo until needed. PVK films were deposited onto the as-prepared steel surfaces as well as ITO through potentiostatic and potentiodynamic (CV) means from 1 mg/mL solutions in CH_2Cl_2 containing 0.1 M TBAP as support electrolyte.

2.2. General Instrumentation. All electrodepositions were performed using a Partsat 2263 potentiostat and Powersuite software (Princeton Applied Research, Inc.). A three-electrode cell system was used with counter, reference, and working electrodes. The counter electrode was a Pt wire, which had been sonicated in 1 M $\text{HCl}_{(aq)}$ for 15 min, rinsed in water, ethanol, and blow-dried. The reference electrode was a nonaqueous Ag/AgCl electrode (0.1 M in acetonitrile), and the working

electrodes were the steel coupons or ITO slides. Potentiostatic electrodeposition was achieved by inducing a constant (0 V) potential for 10 s, then stepping it to 1.2 V for 1000 s. CV-driven electrodeposition was performed by cycling the potential between 0 and 1.4 V at a scan rate of 50 mV s $^{-1}$ for 20 cycles. After each electrochemical deposition, PVK films were carefully rinsed with CH_2Cl_2 dropwise to remove any unbound/physically adsorbed material, dried under delicate N_2 stream, and stored in vacuo at room temperature.

Atomic force microscopy (AFM) images were obtained in MAC mode with a PicoPlus PicoScan 1500 (Agilent Technologies formerly Molecular Imaging, Inc.) at 21°C and 50% humidity. The lever tip was a Molecular Imaging type II MAC (spring constant = 2.8 N m^{-1} , resonance frequency = 75 kHz), and the scan rate was 10 000 nm s $^{-1}$. All image processing was performed with SPIP evaluation software (Scanning Probe Image Processor, Image Metrology).

X-ray photoelectron spectroscopy (XPS) was done using a Physical Electronics 5700 instrument with photoelectrons generated by a nonmonochromatic Al K α irradiation (1486.6 eV). Photoelectrons were collected at a takeoff angle of 45° using a hemispherical analyzer operated in the fixed retard ratio mode (energy resolution setting = 11.75 eV). The binding energy scale was calibrated before analysis using the Cu 2p $_{3/2}$ and Ag 3d $_{5/2}$ lines. Charge neutralization was ensured through cobombardment of the irradiated area with an electron beam and the aforementioned nonmonochromatic Al K α source, placing the C 1s peak at a binding energy of 284.6 (0.2) eV.

FT-IR spectra were recorded with a FTS 7000 Digilab spectrometer within the $3500\text{--}750 \text{ cm}^{-1}$ range in multiple attenuated total reflection (ATR) geometry at the surface of the waveguide prism (ZnSe window, transmits down to 650 cm^{-1}) equipped with a liquid N_2 -cooled MCT detector.

Electrochemical impedance spectroscopy (EIS), in the absence of redox species, was used to estimate the corrosion-protection performance of PVK coatings against aqueous NaCl.⁵⁶ Impedance data were collected after 48 h 8 and 6 days (Supporting Information) of immersion of steel samples in 0.5 M aqueous NaCl. An Autolab PGSTAT12 potentiostat equipped with Frequency Response Analyzer (FRA) Eco Chemie B.V. software (Utrecht, The Netherlands) was utilized, along with a three-electrode cell, which consisted of an aqueous Ag/Ag $^+$ reference electrode (3.5 M in NaCl), a platinum wire as counter electrode, and the coated steel sample (geometry area of ca. 1.0 cm^2) as a working electrode. Applied sinusoidal perturbations of 10 mV were in the frequency range 100 kHz–10 mHz.

3. Results and Discussion

3.1. Electrochemical Coating Fabrication. Electrodeposition of PVK coatings was carried out by either potentiostatic or potentiodynamic (CV) methods. The current versus time (potentiostatic) curves for PVK deposition on steel coupons are shown in Figure 2a. Potentiostatic deposition of carbazole-based polymers is thought of as strongly dependent on substrate preparation, applied voltage, and nucleation rate.⁷¹ For these reasons, a step potential up to 1.2 V 72 with a long period was applied, to ensure a thorough coverage of the working electrodes because no specific/advanced surface treatments were implemented on them. On the other hand, the potentiodynamic electrodeposition on steel (Figure 2b) displayed an oxidation onset at ca. 0.7 V (vs Ag/Ag $^+$), which is in the typical range for CV-driven electropolymerization of PVK.⁶³ Successive waves yielded higher anodic current peaks with corresponding cathodic peaks. Hence, the anodic scans correspond to oxidation

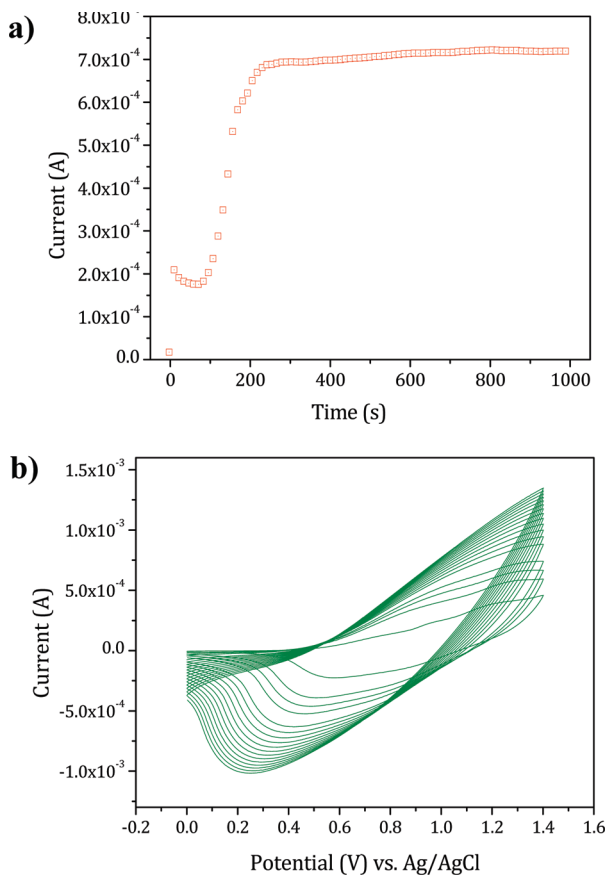


Figure 2. Potentiostatic (a, constant potential of +1.2 V) and potentiodynamic (b, 20 cycles at 50 mV s⁻¹) electrodepositions of PVK on steel coupons from solution (1 mg/mL in CH₂Cl₂) vs Ag/AgCl.

of the carbazole unit⁷³ to give the carbazyl radical cation, which, upon cathodic scan, pairs up with another carbazyl moiety adjacent to it to form a dimer. Subsequent current increase (both anodic and cathodic) explains that the process is iterated to give dimers, trimers, oligomers, and eventually cross-linked film that deposits on the working electrode. Note that the process can proceed by either inter- or intramolecular cross-linking.^{74–76} In all the cases, the films were visibly uniform over either substrate.

3.2. Coating Characterization – IR and XPS. Attenuated total reflection (ATR) infrared spectroscopy of the coatings^{77,78} on ITO support was utilized to analyze the two types of methods for fabricating PVK films: potentiostatic and CV depositions. The films were mounted on a ZnSe crystal in an ATR experiment, and spectra were obtained (Figure 3). Both showed the reported vibrational modes of PVK (carbazole): double bands (indicating a 1:2 disubstituted benzene rings) at circa at 730 and 750 cm⁻¹, C–N stretches at ca. 1230 and 1330 cm⁻¹, aromatic C=C absorptions at 1470 and 1600 cm⁻¹, and the C–H stretch at ca. 3060 cm⁻¹, which are typical for PVK.⁷⁹ This indicated that the CPN PVK films can be fabricated using both methods to give identical compositions. XPS, a surface-sensitive analytical technique, was chosen for investigating the elemental composition of the PVK films (Figure 4) on ITO supports. From high-resolution XPS scans, the calculated ratio of carbon to nitrogen in the polymer was found to be 14:1, which is consistent with the carbon-to-nitrogen ratio expected for PVK. Furthermore, the In and O peaks are still present, indicating a relatively thin film structure on the ITO substrate. Both IR and

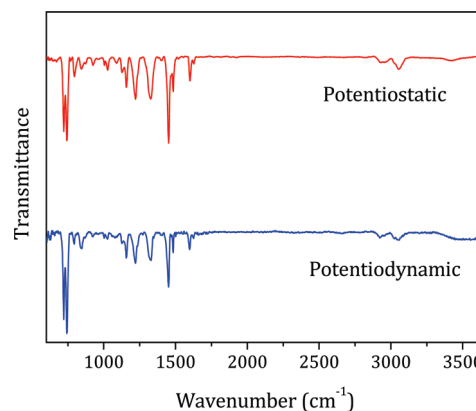


Figure 3. ATR infrared spectra of PVK films electrodeposited on ITO by potentiostatic and CV means. Nominal spectral resolution: 4 cm⁻¹.

XPS data confirmed the spectral data and distribution in the binding energy associated with the cross-linking of the carbazole units.⁶⁴

3.3. Atomic Force Microscopy Studies. AFM analysis was done on the PVK film samples deposited on steel through either potentiostatic or potentiodynamic methods. Figure 5 gives the 2-D and 3-D (inset) topographies of bare steel, whose surface was scanned as control experiment to retrieve information about coating smoothness. Its average roughness (rms) was less than 10 nm, a value lower than that of either coating (vide infra).

In Figures 6 and 7, the AFM images of the PVK coatings (potentiostatic and CV-driven, respectively) vividly showed higher surface roughness and with different domain sizes. This is not surprising, because no polishing and/or pickling of the steel coupons was carried out. Hence, the substrates retained their asperity, which, upon polymer deposition, increased.

It was decided not to implement ulterior surface pretreatments on the steel samples because of the aim to evaluate film deposition under native conditions. Together with the change in morphology and the increase in rms roughness value, deposition of the films on steel was confirmed. Lower rms values of the CV-deposited, PVK coatings indicated less roughness, implying that the films deposited by potentiostatic were rougher than the corresponding CV-deposited films. Thus, the results showed that the film roughness increased upon changing the deposition method; that is, potentiostatic deposition of PVK on steel produced rougher surfaces. However, reasonably smooth PVK films can be deposited by potentiodynamic means on steel. The task is not a trivial one, because the deposition methodology becomes crucial when delamination/exfoliation tests are conducted⁸⁰ for anticorrosion purposes.⁸¹ Comparison of potentiostatic and potentiodynamic methods was investigated previously by Herrasti et al.⁸² Poly(aniline) and poly(pyrrole) depositions and their doping with Zn microparticles were compared as anticorrosion coatings on mild steel. However, no morphological studies were reported. In their case, the best coatings were the ones deposited on top of a passivated (by oxide layer) surface.

Electrodeposition of conducting polymers on active metals often proceeds through various mechanisms,⁸³ and the behavior of the polymer layer depends on a number of conditions such as applied voltage, temperature, electrolyte and its concentration, counterion, etc.^{84,85} Often there is competition between 2-D versus 3-D growth of the polymer. Nonaqueous conditions were chosen, because the kinetics of metal dissolution (or its passivation) can be effectively slowed.⁸⁴ In practice, the advantage of using CH₂Cl₂ as electrodeposition medium lies in the solubility of the starting materials, because the PVK

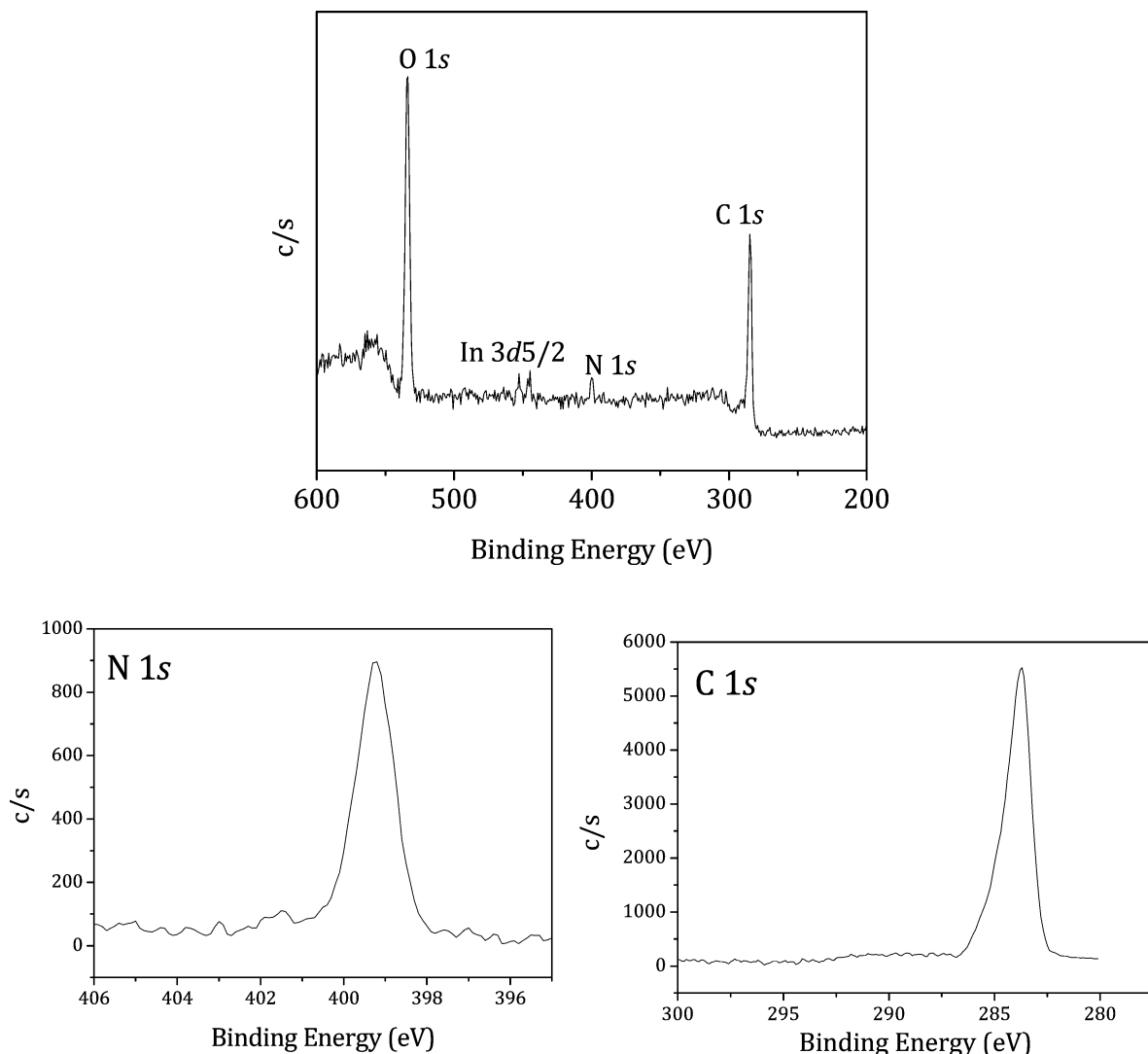


Figure 4. Survey (a) and high-resolution (b,c) XPS scans of the PVK film on ITO support used for identifying the C-to-N composition ratios.

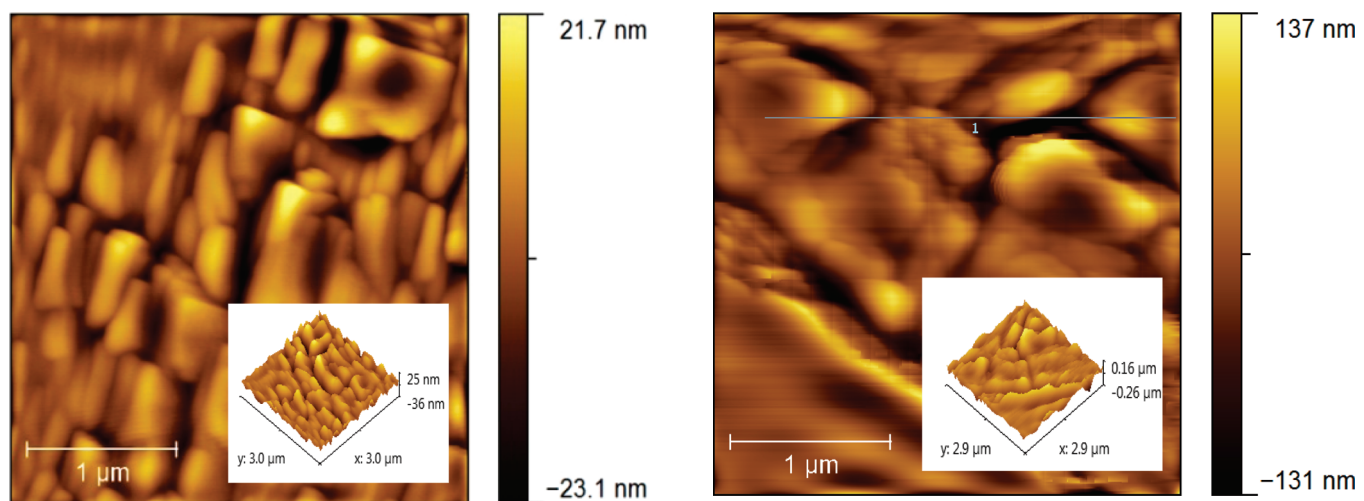


Figure 5. Topographical 2-D and 3-D (inset) AFM images of freshly cleaned, bare steel ($3 \times 3 \mu\text{m}$ scan area). The average rms is 6.57 nm.

concentration can be augmented to favor faster formation of the polymer layer on the substrates. It is possible to optimize the rate of film formation and desired morphology by varying any of the conditions mentioned above. This can be the subject of further studies with this approach.

Figure 6. Topographical 2-D and 3-D (inset) AFM images of potentiostatically deposited PVK on steel ($3 \times 3 \mu\text{m}$ scan area). The average rms is 39.9 nm.

3.4. EIS Studies. Electrochemical impedance analysis (EIS) is a more recent and informative analytical tool⁷ for corrosion studies of organic/polymer coatings on active metals. In its simplest depiction, a metal coated with a coating is connected to an AC source in an electrolyte solution. The electrochemical (0.5

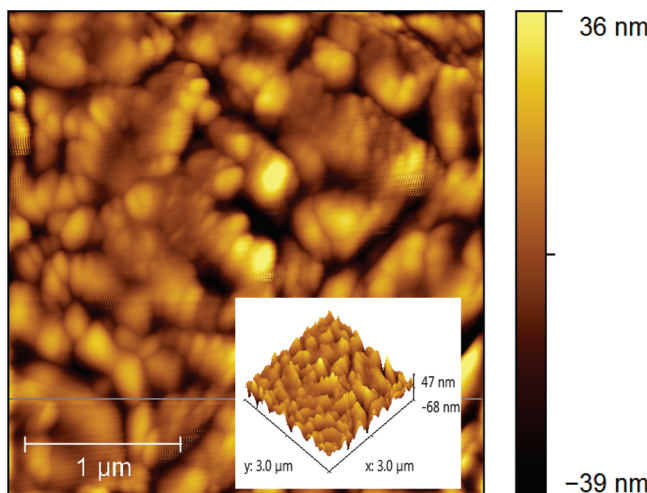


Figure 7. Topographical 2-D and 3-D (inset) AFM images of CV-deposited PVK on steel ($3 \times 3 \mu\text{m}$ scan area). The average rms is 13.0 nm.

or 0.05 M aqueous NaCl) provides ideal conditions for accelerated corrosion tests, as outlined in previous articles⁸ and reviews.⁶⁹ Typical coatings used for corrosion protection have shown⁸⁶ that the diffusion rate of H_2O and O_2 exceeds the limiting value for oxygen reduction. However, the same coatings also displayed very small ion solubility within the polymer matrix (due to the low dielectric constant values). Other issues that recently arose involve the effectiveness of accelerated corrosion tests on protective coatings.⁹ Although effective for comparing different protective layers among each other, they cannot give information on the mechanism of protection. Insight about self-healing capabilities or adhesion properties cannot be inferred either. Nevertheless, EIS furnishes a measure of the resistance of a coating to ion transport phenomena and can thus shed light on long-term corrosion-related issues. It is a very sensitive detector on the condition of a coated metal, meaning impedance data can indicate changes in the coating long before any visible damage occurs.⁸⁷

The impedance Z of a coating placed between an electrolyte solution and an electrode is characterized by its magnitude $|Z|$ ($\Omega \text{ cm}^2$) and phase angle ϕ (deg) as functions of the frequency f . The former quantity gives its absolute value (the higher is Z , the higher is the dielectric behavior of the coating), while the latter expresses the balance between capacitive (Z'') and resistive (Z') behavior of the coating. Clearly, a highly capacitive material will allow more efficient charge separation between the capacitor plates, therefore raising the insulating features of the coating itself. These, in turn, are strongly dependent upon the coating smoothness: indeed, rough surface morphologies are more likely to create local defects, pinholes, and crevices whereupon corrosion may start at appreciable rates. For this reasons, impedance analysis was carried out on the smoothest coating fabricated, the CV-deposited PVK film. The effect of a small (10 mV) sinusoidal voltage on it after 48 h of immersion in 0.5 M aqueous NaCl is shown in Bode (Figure 8a and b) and Nyquist (Figure 9) plots. For PVK, the Bode phase plot (Figure 8a) shows that the phase angle ϕ is larger than 87° in the high-to-mid frequency range ($10^{-1} \text{ Hz} < f < 10 \text{ Hz}$). The slope of the Bode plot (Figure 8b) is -1 within the $10^{-2} \text{ Hz} < f < 10^2 \text{ Hz}$ range. This may be interpreted as an ionic insulation under the current conditions; the PVK film does not allow ionic transport to occur in a facile way over the time scale of the experiment.⁸⁸ Moreover, a look at $|Z|$ at high frequencies shows large values (ca. $10^6 \Omega \text{ cm}^2$), which, according to standard

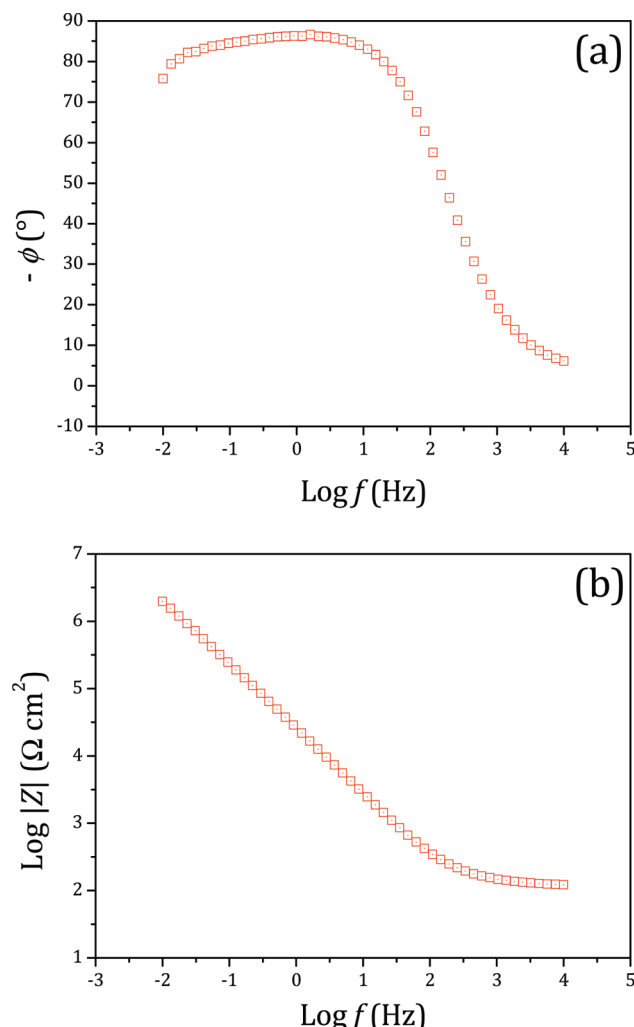


Figure 8. Bode phase (a) and Bode plot (b) for PVK coatings on steel coupons, potentiodynamic depositions.

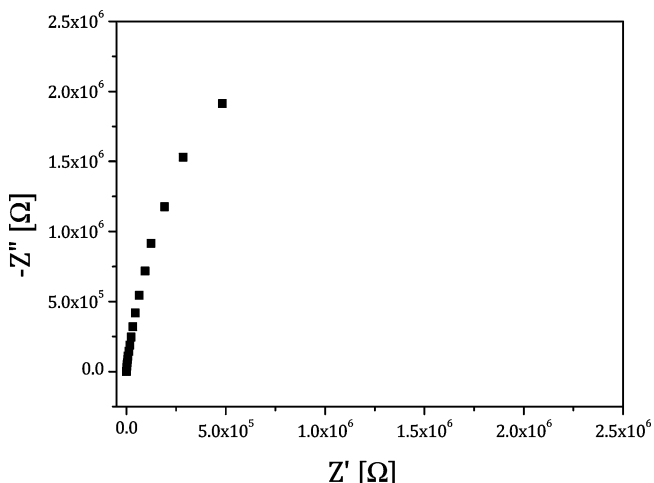


Figure 9. Nyquist plot for PVK coating on a steel coupon, potentiodynamic deposition.

criteria, indicates a good protection against corrosion and an overall reasonably good coating.⁸⁹

Such a behavior of the PVK film does not resemble an ideal dielectric medium interposed between the parallel plates of a capacitor (Helmholtz's ideal capacitor),⁹⁰ because it does not afford a pure capacitive behavior. However, according to Grundenmeier et al.,⁶⁹ it can be reasonably likened to a quasi-

ideal coating, which does not exhibit corrosion attack, at least under the experimental conditions. On the other hand, a hybrid PVK/silica coating afforded a different, lower set of ϕ and $|Z|$ values (CV-deposited hybrid films) (Supporting Information). Moreover, the scattered phase angle data points at high frequencies have been interpreted as the beginning of the corrosion process in hybrid systems.⁵⁶ Similar studies were also done with a longer duration of exposure to the corrosive NaCl solution environment (6 days). The results showed a further degradation of the coating effectiveness with longer periods of exposure (Supporting Information). Note that EIS is most effective for investigating long-term corrosion mechanisms.

Ulterior analysis of the PVK film was retrieved from the Z' versus Z'' complex plane (Nyquist plot, Figure 9). In an ideal capacitor, the real part of the impedance is only related to the solution resistance R_s , whereas the imaginary part is related to the capacitance C as $Z'' = -1/(i\omega C)$, ω being the excitation pulse. The Nyquist plot of the PVK film exhibited tilting, meaning a departure from the perfect insulator behavior: this implies imperfect coverage of the metal surface; as Z' increases, the resistive behavior of the polymer layer increases as well. When $Z' = 0$, the ideal capacitor has purely imaginary impedance, and thus its Nyquist plot should yield a vertical line parallel to the imaginary axis in the complex plane. In other words, a purely resistive behavior implies $\phi = 0$, while purely capacitive behavior (i.e., no energy dissipation on the coating, true dielectric behavior) implies $\phi = \pi/2$.⁹¹

In the case of the PVK coating, the Nyquist plot confirms the Bode data in that a non-uniform coverage is present on the steel coupon. From Figure 8a, ϕ does not reach a maximum over the whole frequency range because it varies with the capacitive and resistive behaviors of the coating contribution. From Figure 8b, ion diffusion (the plateau at ca. $10^2 \Omega \text{ cm}^2$) occurs at low f values,⁹² and this is visible in the Nyquist plot as well, indicating a departure from purely capacitive behavior of the PVK coating.

However, by inspecting the two sets of data, a PVK coating is still very much a suitable candidate for anticorrosion applications. The $|Z|$ and ϕ values fall in the required range of good dielectric coatings for anticorrosion use.^{89,90,93} Although rough in surface morphology with steel, a CV-deposited PVK film is still a promising alternative to other CPs for corrosion protection. Visual corrosion tests on PVK films deposited by potentiostatic means on steel were attempted (Supporting Information) but eventually with poor adhesion in the presence of NaCl media. However, the differences between the corroded (brown) unprotected steel coupon control and the PVK-coated steel coupon (green coating) are very clear. Further studies can be made to optimize the parameters for visual corrosion tests.

In summary, the corrosion resistance of a PVK coating, from the above results, can be attributed to its properties as a physical barrier for corrosion. PVK because of the polyvinylidic backbone has better film-forming properties from solution than the direct electrodeposition of monomers, a precipitation process. The flexible conformation of the polymer chains ($T_g > 250^\circ\text{C}$),⁹⁴ along with their subsequent immobilization upon electrochemical cross-linking of the carbazole pendant units, can act as an effective barrier to ion diffusion. Under optimized experimental conditions, the CPN approach may furnish a good method for depositing CP films onto metallic substrates. The intimate entanglement and cross-linking of the Cbz units seems to be effective toward dielectric insulation of the underneath metal as proven by EIS and visual inspection. Furthermore, ulterior

implementation of surface treatments (e.g., metal pickling)⁹⁵ should be effective for improved adhesion properties of the coating.

4. Conclusions

PVK coatings were successfully fabricated and deposited on steel coupons and ITO glasses. Potentiostatic and potentiodynamic electrodeposition afforded CPN films whose main feature was the presence of cross-linked oligo- and polycarbazole units. Electrodeposition on ITO revealed a well-behaved electrochemical system with good constant current saturation (potentiostatic) and cyclic stability (CV). The formation of a cross-linked carbazole containing film was confirmed by IR and XPS measurements. Morphological characterization of these films by AFM indicated higher surface roughness when potentiostatic electrodeposition was performed. This should provide another variable for CPN film deposition in which anticorrosion tests showed the best performance being attained from CV-deposited PVK films on steel coupons. In general, EIS data showed promising anticorrosion behavior for such coatings, and data simulation (i.e., fitting into suitable equivalent circuits) is underway.

Acknowledgment

We acknowledge technical support from Agilent Technologies, Biolin Scientific Inc., and Metrohm.

Supporting Information Available: EIS and visual corrosion tests for the PVK-coated steel coupons. EIS experiments for PVK/silica coatings. Mechanism for carbazole and PVK electropolymerization. This material is available free of charge via the Internet at <http://pubs.acs.org>.

Literature Cited

- (1) Tallman, D. E.; Bierwagen, G. P. *Handbook of Conducting Polymers*; CRC Press: Boca Raton, FL, 2007.
- (2) Magnussen, O. Corrosion Protection by Inhibition. In *Corrosion and Oxide Films*; Stratmann, M., Frankel, G. S., Eds.; Wiley-VCH Verlag GmbH & Co. KGaA: Weinheim, Germany, 2003.
- (3) Corrosion costs and preventative strategies in the United States. Tech Brief FHWA-RD-01-157, US Dept. of Transportation, 2002.
- (4) Osborne, J. H. Observations on Chromate Conversion Coatings from a Sol-Gel Perspective. *Prog. Org. Coat.* **2001**, *41*, 280–286.
- (5) Twite, R. L.; Bierwagen, G. P. Review of Alternatives to Chromate for Corrosion Protection of Aluminum Aerospace Alloys. *Prog. Org. Coat.* **1998**, *33*, 91–100.
- (6) Cohen, S. M. Replacements for Chromium Pretreatments on Aluminum. *Corrosion* **1995**, *51*, 71–78.
- (7) Orazem, M. E.; Tribollet, B. *Electrochemical Impedance Spectroscopy*; Wiley-Interscience: New York, 2008.
- (8) Shchukin, D. G.; Zheludkevich, M.; Yasakau, K.; Lamaka, S.; Ferreira, M. G. S.; Möhwald, H. Layer-by-Layer Assembled Nanocontainers for Self-Healing Corrosion Protection. *Adv. Mater.* **2006**, *18*, 1672–1678.
- (9) Zheludkevich, M.; Yasakau, K.; Bastos, A. C.; Karavai, O. V.; Ferreira, M. G. S. On the Application of Electrochemical Impedance Spectroscopy to Study the Self-Healing Properties of Protective Coatings. *Electrochim. Commun.* **2007**, *9*, 2622–2628.
- (10) Schmidt, H.; Langenfeld, S.; Naß, R. A New Corrosion Protection Coating System for Pressure-Cast Aluminium Automotive Parts. *Mater. Des.* **1997**, *18*, 309–313.
- (11) Zheludkevich, M. L.; Serra, R.; Montemor, M. F.; Yasakau, K. A.; Miranda Salvado, I. M.; Ferreira, M. G. S. Nanostructured Sol-gel Coatings Doped with Cerium Nitrate as Pre-treatments for AA2024-T3: Corrosion Protection Performance. *Electrochim. Acta* **2005**, *51*, 208–217.
- (12) Macdonald, D. D.; McKubre, M. C. H. In *Impedance Spectroscopy Theory, Experiment, and Applications*; Barsoukov, E., Macdonald, J. R., Eds.; John Wiley & Sons, Inc.: Hoboken, NJ, 2005.

- (13) Brooman, E. W. Modifying Organic Coatings to Provide Corrosion Resistance: Part I—Background and General Principles. *Met. Finish.* **2002**, *100*, 44–47.
- (14) Brooman, E. W. Modifying Organic Coatings to Provide Corrosion Resistance: Part II—Inorganic Additives and Inhibitors. *Met. Finish.* **2002**, *100*, 48–52.
- (15) MacDiarmid, A. G. *Short Course on Conductive Polymers*; SUNY, New Platz: New York, 1985.
- (16) Arbizzani, C.; Mastragostino, M. An Overview of n-doped Conjugated Polymers. *Current Trends in Polymer Science*; Research Trends: Trivandrum, 1997.
- (17) Epstein, A. J. Theory and Simulations of Polymer Surfaces and Interfaces. *MRS Bull.* **1997**, *22*, 16–23.
- (18) Heeger, A. J. Semiconducting and Metallic Polymers: The Fourth Generation of Polymeric Materials. *J. Phys. Chem. B* **2001**, *105*, 8475–8491.
- (19) Heinze, J. A Brief History of Photoinduced Electron Transfer and Related Reactions. *Top. Curr. Chem.* **1990**, *152*, 1–47.
- (20) Amaria, M. N. *Proc. Electrochem. Soc.* **2003**, *27*, 532–544.
- (21) Heeger, A. J. Nobel Lecture: Semiconducting and Metallic Polymers: The Fourth Generation of Polymeric Materials. *Rev. Mod. Phys.* **2001**, *73*, 681–700.
- (22) Petr, A.; Zhang, F.; Peisert, H.; Knupfer, M.; Dunsch, L. Electrochemical Adjustment of the Work Function of a Conducting Polymer. *Chem. Phys. Lett.* **2004**, *385*, 140–143.
- (23) Nazarov, A. P.; Thierry, D. Scanning Kelvin Probe Study of Metal/Polymer Interfaces. *Electrochim. Acta* **2004**, *49*, 2955–2964.
- (24) Wallace, G. G.; Spinks, G. M.; Kane-Maguire, L.; Teasdale, P. R. *Conductive Electroactive Polymers: Intelligent Materials Systems*, 2nd ed.; CRC Press LLC: Boca Raton, FL, 2002.
- (25) de Souza, S.; Pereira da Silva, J. E.; Córdoba de Torresi, S. I.; Temperini, M. L. A.; Torresi, R. M. Polyaniline-based Acrylic Blends for Iron Corrosion Protection. *Electrochim. Solid-State Lett.* **2001**, *4*, B27–B30.
- (26) Tallman, D. E.; Pae, Y.; Bierwagen, G. P. Scanning Vibrating Electrode Studies of Electroactive Conducting Polymers on Active Metals. In *Electroactive Polymers for Corrosion Control*; Zarras, P., Stenger-Smith, J. D., Wei, Y., Eds.; American Chemical Society: Washington, DC, 2003.
- (27) Thompson, K. G.; Benicewicz, B. C. Corrosion-protective Coatings from Electroactive Polymers. In *Electroactive Polymers for Corrosion Control*; Zarras, P., Stenger-Smith, J. D., Wei, Y., Eds.; American Chemical Society: Washington, DC, 2003.
- (28) Dominis, A. J.; Spinks, G. M.; Wallace, G. G. Comparison of Polyaniline Primers Prepared with Different Dopants for Corrosion Protection of Steel. *Prog. Org. Coat.* **2003**, *48*, 43–49.
- (29) Kinlen, P. J.; Graham, C. R.; Ding, Y. Electroactive Polymers & Smart Coatings for Corrosion Inhibition of Aluminum Alloys. *Polym. Prepr. (Am. Chem. Soc., Div. Polym. Chem.)* **2004**, *45*, 146–147.
- (30) Kinlen, P. J.; Ding, Y.; Silverman, D. C. Past, Present and Future ‘Smart’ Protective Coatings. *Corrosion* **2002**, *58*, 490–497.
- (31) Kendig, M.; Hon, M. Environmentally Triggered Release of Oxygen-reduction Inhibitors from Inherently Conducting Polymers. *Corrosion* **2004**, *60*, 1024–1030.
- (32) Torresi, R. M.; de Souza, S.; Pereira da Silva, J. E.; Córdoba de Torresi, S. I. Galvanic Coupling Between Metal Substrate and Polyaniline Acrylic Blends: Corrosion Protection Mechanism. *Electrochim. Acta* **2005**, *50*, 2213–2218.
- (33) Kendig, M.; Hon, M.; Warren, L. Smart Corrosion Inhibiting Coatings. *Prog. Org. Coat.* **2003**, *47*, 183–189.
- (34) Aparicio, M.; Klein, L. C. Thin and Thick RuO₂-TiO₂ Coatings on Titanium Substrates by the Sol-gel Process. *J. Sol-Gel Sci. Technol.* **2004**, *29*, 81–88.
- (35) Fukuda, H.; Matsumoto, Y. Formation of Ti-Si Composite Oxide Films on Mg-Al-Zn Alloy by Electrophoretic Deposition and Anodization. *Electrochim. Acta* **2005**, *50*, 5329–5333.
- (36) Shen, G. X.; Chen, Y. C.; Lin, C. J. Corrosion Protection of 316 L Stainless Steel by a TiO₂ Nanoparticle Coating Prepared by the Sol-gel Method. *Thin Solid Films* **2005**, *489*, 130–136.
- (37) Yun, H.; Li, J.; Chen, H.-B.; Lin, C.-J. A Study on the N-, S- and Cl-modified Nano-TiO₂ Coatings for Corrosion Protection of Stainless Steel. *Electrochim. Acta* **2007**, *52*, 6679–6685.
- (38) Shchukin, D.; Möhwald, H. Surface-engineered Nanocontainers for Entrapment of Corrosion Inhibitors. *Adv. Funct. Mater.* **2007**, *17*, 1451–1458.
- (39) Lamaka, S. V.; Zheludkevich, M. L.; Yasakau, K. A.; Serra, R.; Poznyak, S. K.; Ferreira, M. G. S. Nanoporous Titania Interlayer as Reservoir of Corrosion Inhibitors for Coatings with Self-healing Ability. *Prog. Org. Coat.* **2007**, *58*, 127–135.
- (40) Zheludkevich, M. L.; Yasakau, K. A.; Poznyak, S. K.; Ferreira, M. G. S. Triazole and Thiazole Derivatives as Corrosion Inhibitors for AA2024 Aluminium Alloy. *Corros. Sci.* **2005**, *47*, 3368–3383.
- (41) Robel, I.; Subramanian, V.; Kuno, M.; Kamat, P. Quantum Dot Solar Cells. Harvesting Light Energy with CdSe Nanocrystals Molecularly Linked to Mesoscopic TiO₂ Films. *J. Am. Chem. Soc.* **2006**, *128*, 2385–2393.
- (42) Nazeeruddin, M. K.; Kay, A.; Rodicio, I.; Humphry, B. R.; Mueller, E.; Liska, P.; VLachopoulos, N.; Graetzel, M. Conversion of Light to Electricity by *cis*-X₂Bis(2,2'-bipyridyl-4,4'-dicarboxylate)ruthenium(II) Charge-transfer Sensitizers (X = Cl[−], Br[−], I[−], CN[−] and SCN[−]) on Nanocrystalline TiO₂ Electrodes. *J. Am. Chem. Soc.* **1993**, *115*, 6382–6390.
- (43) Meyer, T. J.; Meyer, G. J.; Pfennig, B. W.; Schoonover, J. R.; Timson, C. J.; Wall, J. F.; Kobusch, C.; Chen, X. H.; Peek, B. M.; Wall, C. G.; Ou, W.; Erickson, B. W.; Bignozzi, C. A. Molecular Level Electron Transfer and Excited State Assemblies on Surface of Metal Oxides and Glass. *Inorg. Chem.* **1994**, *33*, 3952–3964.
- (44) Schroeder, S. *Eur. Coat. J.* **2000**, *76*, 51–58.
- (45) Khramov, A. N.; Voevodin, N. N.; Balbyshev, V. N.; Donley, M. S. Hybrid Organo-ceramic Corrosion Protection Coatings with Encapsulated Organic Corrosion Inhibitors. *Thin Solid Films* **2004**, *447*, 549–557.
- (46) Schubert, U. Chemical Modification of Titanium Alkoxides for Sol-gel Processing. *J. Mater. Chem.* **2005**, *15*, 3701–3715.
- (47) Kasten, L. S.; Grant, J. T.; Grebasch, N.; Voevodin, N.; Arnold, F. E.; Donley, M. S. An XPS Study of Cerium Dopants in Sol-gel Coatings for Aluminum 2024-T3. *Surf. Coat. Technol.* **2001**, *140*, 11–15.
- (48) Qafsaoui, W.; Huet, F.; Takenouti, H. Analysis of the Inhibitive Effect of BTAH on Localized Corrosion of Al 2024 from Electrochemical Noise Measurements. *J. Electrochem. Soc.* **2009**, *156*, C67–C74.
- (49) Kongkanand, A.; Tvrdy, K.; Takechi, K.; Kuno, M.; Kamat, P. V. Quantum Dot Solar Cells. Tuning Photoresponse through Size and Shape Control of CdSe-TiO₂ Architecture. *J. Am. Chem. Soc.* **2008**, *130*, 4007–4015.
- (50) Yi, C.; An, Y. Nanometer Modified Epoxy Sealing Paint and Its Preparation. Chinese Patent 1887992, 2007.
- (51) Roberge, P. R. *Corrosion Engineering: Principles and Practice*; McGraw-Hill: New York, 2008.
- (52) Shibata, T.; Takeyama, T. Pitting Corrosion as a Stochastic Process. *Nature (London)* **1976**, *260*, 315–316.
- (53) Shibata, T.; Takeyama, T. Stochastic Theory of Pitting Corrosion. *Corrosion (Houston)* **1977**, *33*, 243.
- (54) Yasakau, K. A.; Zheludkevich, M. L.; Karavai, O. V.; Ferreira, M. G. S. Influence of Inhibitor Addition on the Corrosion Protection Performance of Sol-gel Coatings on AA2024. *Prog. Org. Coat.* **2008**, *63*, 352–361.
- (55) Yang, H.; van Ooij, W. J. Plasma Deposition of Polymeric Thin Films on Organic Corrosion-inhibiting Paint Pigments: A Novel Method to Achieve Slow Release. *Plasmas Polym.* **2003**, *8*, 297–323.
- (56) Palanivel, V.; Huang, Y.; van Ooij, W. J. Effect of Addition of Corrosion Inhibitors to Silane Films on the Performance of AA2024-T3 in a 0.5 M NaCl Solution. *Prog. Org. Coat.* **2005**, *53*, 153–168.
- (57) Fulghum, T. M.; Patton, D. L.; Advincula, R. C. Fuzzy Ternary Particle Systems by Surface-Initiated Atom Transfer Radical Polymerization from Layer-by-Layer Colloidal Core-Shell Macroinitiator Particles. *Langmuir* **2006**, *22*, 8397–8402.
- (58) Taranekar, P.; Baba, A.; Fulghum, T. M.; Advincula, R. Conjugated Polymer Network Films from Precursor Polymers: Electrocopolymerization of a Binary Electroactive Monomer Composition. *Macromolecules* **2005**, *38*, 3679–3687.
- (59) Advincula, R. Nanostructured Conjugated Polymer Network Ultrathin Films Using the Precursor Polymer Approach. *J. Coat. Technol.* **2008**, *5*, 34–37.
- (60) Deng, S.; Advincula, R. C. Polymethacrylate Functionalized Polypyrrole Network Films on Indium Tin Oxide: Electropolymerization of a Precursor Polymer and Comonomer. *Chem. Mater.* **2002**, *14*, 4073–4080.
- (61) Roitman, D. B.; Inaoka, S.; Advincula, R. Processor Polymers for the Electrochemical Deposition of Electrically Conducting Polymer Films. U.S. Patent 6,552,101, 2003.
- (62) Xia, C.; Advincula, R. C.; Baba, A.; Knoll, W. Electrochemical Patterning of a Polyfluorene Precursor Polymer from a Microcontact Printed (μ CP) Monolayer. *Chem. Mater.* **2004**, *16*, 2852–2856.
- (63) Baba, A.; Onishi, K.; Knoll, W.; Advincula, R. Investigating Work Function Tunable Hole-Injection Transport Layers of Electrodeposited Polycarbazole Network Thin Films. *J. Phys. Chem. B* **2004**, *108*, 18949–18955.
- (64) Fulghum, T. M.; Taranekar, P.; Advincula, R. C. Grafting Hole-transport Precursor Polymer Brushes on ITO Electrodes: Surface-initiated

Polymerization and Conjugated Polymer Network Formation of PVK. *Macromolecules* **2008**, *41*, 5681–5687.

(65) Shirota, Y.; Kakuta, T.; Kanega, H.; Mikawa, H. Rectification and Photovoltaic Properties of a Schottky Barrier Cell Using Electrochemically-doped Poly(*N*-vinylcarbazole). *Chem. Commun.* **1985**, 1201–1202.

(66) Park, Y.; Taranekar, P.; Park, J.-Y.; Fulghum, T. M.; Baba, A.; Ponnapati, R.; Advincula, R. Hybrid CdSe Nanoparticle-Dendron Boxes: Electropolymerization and Energy-transfer Mechanism Shift. *Adv. Funct. Mater.* **2008**, *18*, 2071–2078.

(67) Thompson, K. G.; Benicewicz, B. C. Corrosion-Protective Coatings from Electroactive Polymers. In *Electroactive Polymers for Corrosion Control*; Zarras, P., Stenger-Smith, J. D., Wei, Y., Eds.; American Chemical Society: Washington, DC, 2003.

(68) Tüken, T.; Yazici, B.; Erbil, M. Electrochemical Synthesis of Polythiophene on Nickel Coated Mild Steel and Corrosion Performance. *Appl. Surf. Sci.* **2005**, *239*, 398–409.

(69) Grundmeier, G.; Schmidt, W.; Stratmann, M. Corrosion Protection by Organic Coatings: Electrochemical Mechanism and Novel Methods of Investigation. *Electrochim. Acta* **2000**, *45*, 2515–2533.

(70) Wang, C.-T.; Chen, S.-H.; Ma, H.-Y.; Qi, C.-S. Protection of Copper Corrosion by Carbazole and *N*-vinylcarbazole Self-assembled Film in NaCl Solution. *J. Appl. Electrochem.* **2003**, *33*, 179–186.

(71) Skompska, M.; Peter, L. M. Electrodeposition and Electrochemical Properties of Poly(*N*-vinylcarbazole) Films on Platinum Electrodes. *J. Electroanal. Chem.* **1995**, *383*, 43–52.

(72) Marrec, P.; Dano, C.; Gueguen-Simonet, N.; Simonet, J. The Anodic Oxidation and Polymerization of Carbazoles and Dicarbazoles *N*-substituted by Polyether Chains. *Synth. Met.* **1997**, *89*, 171–179.

(73) Ambrose, J. F.; Nelson, R. F. Anodic Oxidation Pathways of Carbazoles. *J. Electrochem. Soc.* **1968**, *115*, 1159–1164.

(74) Xia, C.; Fan, X.; Park, M.-K.; Advincula, R. C. Ultrathin Film Electrodeposition of Polythiophene Conjugated Networks through a Polymer Precursor Route. *Langmuir* **2001**, *17*, 7893–7898.

(75) Inaoka, S.; Advincula, R. Synthesis and Oxidative Cross-linking of Fluorene-containing Polymers to Form Conjugated Network Polyfluorenes: Poly(fluoren-9,9-diyl-*alt*-alkan- α,ω -diyl). *Macromolecules* **2002**, *35*, 2426–2428.

(76) Taranekar, P.; Fan, X.; Advincula, R. Distinct Surface Morphologies of Electropolymerized Polymethylsiloxane Network Polypyrrole and Comonomer Films. *Langmuir* **2002**, *18*, 7943–7952.

(77) He, R.; Qian, X.-F.; Yin, J.; Bian, L.-J.; Xi, H.-a.; Zhu, Z.-k. In situ synthesis of CdSe/PVK Nanocomposites and Their Optical Properties. *Mater. Lett.* **2003**, *57*, 1351–1354.

(78) Rivaton, A.; Mailhot, B.; Derderian, G.; Bussiere, P. O.; Gardette, J.-L. Investigation of the Photophysical Processes and Photochemical Reactions Involved in PVK Films Irradiated at $\lambda > 300$ nm. *Macromolecules* **2003**, *36*, 5815–5824.

(79) Ling, Q.-D.; Lim, S.-L.; Song, Y.; Zhu, C.-X.; Chan, D. S.-H.; Kang, E.-T.; Neoh, K. G. Nonvolatile Polymer Memory Device Based on Bistable Electrical Switching in a Thin Film of Poly(*N*-vinylcarbazole) with Covalently Bonded C₆₀. *Langmuir* **2007**, *23*, 312–319.

(80) Yeh, J.-M.; Weng, C.-J.; Liao, W.-J.; Mau, Y.-W. Anticorrosively Enhanced PMMA-SiO₂ Hybrid Coatings Prepared from the Sol-gel Approach with MSMA as the Coupling Agent. *Surf. Coat. Technol.* **2006**, *20*, 1788–1795.

(81) Rammelt, U.; Nguyen, P. T.; Plieth, W. Protection of Mild Steel by Modification with Thin Films of Polymethylthiophene. *Electrochim. Acta* **2001**, *46*, 4251–4257.

(82) Herrasti, P.; Recio, F. J.; Ocón, P.; Fatás, E. Effect of the Polymer Layers and Bylayers on the Corrosion Behaviour of Mild Steel: Comparison with Polymers Containing Zn Microparticles. *Prog. Org. Coat.* **2005**, *54*, 285–291.

(83) Biallozor, S.; Kupniewska, A. Conducting Polymers Deposited on Active Metals. *Synth. Met.* **2005**, *155*, 443–449.

(84) Simonet, J.; Rault-Berhetot, J. Electrochemistry: A Technique to Form, to Modify, and to Characterize Organic Conducting Polymers. *Prog. Solid State Chem.* **1991**, *21*, 1–10.

(85) Inzelt, G.; Pineri, M.; Schultze, J. W.; Vorotyntsev, M. A. Electron and Proton Conducting Polymers: Recent Developments and Prospects. *Electrochim. Acta* **2000**, *45*, 2403–2421.

(86) Feser, R.; Stratmann, M. Neue Erkenntnisse zum Korrosionsschutz von organischen Beschichtungen auf Eisen. *Werkst. Korros.* **1991**, *42*, 187–195.

(87) MacDonald, J. R. *Impedance Spectroscopy: Emphasizing Solid Materials and Systems*; Wiley-Interscience Publications: New York, 1987.

(88) Park, M.-K.; Lee, D.-C.; Liang, Y.; Lin, G.; Yu, L. Defect-Free Polymer Multilayers Prepared via Chemoselective Immobilization. *Langmuir* **2007**, *23*, 4367–4372.

(89) Bacon, R. C.; Smith, J. J.; Rugg, F. M. Electrolytic Resistance in Evaluating Protective Merit of Coatings on Active Metals. *Ind. Eng. Chem.* **1948**, *40*, 161–167.

(90) Vreugdenhil, A. J.; Balbyshev, V. N.; Donley, M. S. Nanostructured Silicon Sol-gel Surface Treatments for AA 2024-T3 Protection. *J. Coat. Technol.* **2001**, *73*, 35–43.

(91) Boubour, E.; Lennox, R. B. Insulating Properties of Self-Assembled Monolayers Monitored by Impedance Spectroscopy. *Langmuir* **2000**, *16*, 4222–4228.

(92) Murray, J. Electrochemical Test Methods for Evaluating Organic Coatings on Metals: An Update. Part III: Multiple Test Parameter Measurements. *Prog. Org. Coat.* **1997**, *31*, 375–391.

(93) Loveday, D.; Peterson, P.; Rodgers, B. Evaluation of Organic Coatings with Electrochemical Impedance Spectroscopy. Part 2: Application of EIS to Coatings. *J. Coat. Technol.* **2004**, *1*, 88–93.

(94) Pielichowski, J. Thermal Studies of Polyvinylcarbazole and Polyvinylidibromocarbazole. *J. Therm. Anal.* **1972**, *4*, 339–341.

(95) Rammelt, U.; Nguyen, P. T.; Plieth, W. Corrosion Protection by Ultrathin Films of Conducting Polymers. *Electrochim. Acta* **2003**, *48*, 1257–1262.

Received for review April 4, 2010
Revised manuscript received August 20, 2010
Accepted August 27, 2010

IE100813T